American Mineralogist, Volume 74, pages 1023–1031, 1989

Estimating the thermodynamic properties (ΔG_f^0 and ΔH_f^0) of silicate minerals at 298 K from the sum of polyhedral contributions

JOHN A. CHERMAK, J. DONALD RIMSTIDT
Department of Geological Sciences, Virginia Polytechnic Institute and State University, Blacksburg, Virginia 24061, U.S.A.

ABSTRACT

Many physical properties of silicate minerals can be modeled as a combination of basic polyhedral units (Hazen, 1985, 1988). It follows that their thermodynamic properties could be modeled as the sum of polyhedral contributions. We have determined, by multiple regression, the contribution of the $^{[4]}Al_2O_3$, $^{[6]}Al_2O_3$, $^{[6]}Al(OH)_3$, $^{[4]}SiO_2$, $^{[6]}MgO$, $^{[6]}Mg(OH)_2$, $^{[6]}CaO$, $^{[8-z]}CaO$, $^{[6-8]}Na_2O$, $^{[8-12]}K_2O$, H_2O, $^{[6]}FeO$, $^{[6]}Fe(OH)_2$, and $^{[6]}Fe_2O_3$ components to the total ΔG_f^0 and ΔH_f^0 of a selected group of silicate minerals. Using these data we can estimate the ΔG_f^0 and ΔH_f^0 of other silicate minerals from a weighted sum of the contribution of each oxide and hydroxide component: $\Delta G_f^0 = \Sigma\, n_i g_i$, and $\Delta H_f^0 = \Sigma\, n_i h_i$, where n_i is the number of moles of the oxide or hydroxide per formula unit and g_i and h_i are the respective molar free energy and enthalpy contribution of 1 mol of each oxide or hydroxide component. The technique outlined here can be used to estimate the thermodynamic properties of many silicate phases that are too complex or too impure to give reliable calorimetric measurements.

Experimentally measured ΔG_f^0 and ΔH_f^0 vs. predicted ΔG_f^0 and ΔH_f^0 for the minerals used in the model have associated average residuals of 0.26% and 0.24%, respectively. Thermodynamic properties of minerals not used in the model but for which there are experimentally determined calorimetric data have average differences between measured and predicted values of 0.25% for ΔG_f^0 for 18 minerals and 0.22% for ΔH_f^0 for 20 minerals.

INTRODUCTION

Clay and zeolite minerals are very important phases in the near-surface environment, and the understanding of their thermodynamic properties is essential to modeling many geochemical processes. But, experimental measurements of the free energy of formation and enthalpy of formation (ΔG_f^0 and ΔH_f^0, respectively) are few because they are difficult to perform. Problems associated with determining thermodynamic properties of clay and zeolite minerals include their chemical complexity and highly variable composition. The estimation technique for ΔG_f^0 and ΔH_f^0 developed here offers a reasonable way to approximate thermodynamic properties of clays and zeolites.

For silicate minerals, many other techniques exist for estimating ΔG_f^0 (Nriagu, 1975; Chen, 1975; Tardy and Garrels, 1974, 1976, 1977; Karpov and Kashik, 1968; Mattigod and Sposito, 1978; La Iglesia and Aznar, 1986; Sposito, 1986) and ΔH_f^0 (Kubaschewski and Alcock, 1979; Hemingway, 1982; Vieillard and Tardy, 1988). A complete discussion here of each technique and associated errors would be quite lengthy; therefore, only a short summary will be presented. The data base used for most of the ΔG_f^0 estimation techniques is based on solubility measurements of clay minerals. In these techniques, the estimation is based on the combined contributions of hydroxide components [i.e., $Si(OH)_4$, $Al(OH)_3$, etc.] rather than both hydroxide and oxide polyhedra. Karpov and Kashik used a multiple linear-regression technique to estimate the ΔG_f^0 contribution of 36 different oxides to the overall ΔG_f^0 of silicate minerals; however they ignored the hydroxide contributions. Tardy and Garrels (1976) developed an expression that describes the difference between ΔG_f^0 of the simple oxide or hydroxide vs. ΔG_f^0 of that same oxide or hydroxide within the silicate structure. This technique was extended further to include ΔH_f^0 (Vieillard and Tardy, 1988). This basic technique of breaking down minerals into their "building block" components is also used in S^0 estimation (Robinson and Haas, 1983; Holland, 1989). Robinson and Haas's S^0 estimates have small errors within the original data set but when applied outside the model data base, the estimates have much larger associated errors. The Robinson and Haas method of estimating entropy could be refined further if hydroxyls were viewed as parts of polyhedral units, and the simple oxide and hydroxide phases were removed from the model, as will be demonstrated later. Holland's estimation technique gives further refinement to the estimation of S^0 by including a volume correction and considering magnetic contributions when estimating entropy.

This paper describes a multiple linear-regression technique to determine the contribution of oxide and hydroxide components to the ΔG_f^0 and ΔH_f^0 of silicate minerals. The technique is based on the observation that silicate minerals have been shown to act as a combination

0003–004X/89/0910–1023$02.00

TABLE 1. Minerals selected for the thermodynamic regression models and the relative contribution of their polyhedral components

Component: Coordination no.:	Al_2O_3 4	Al_2O_3 6	$Al(OH)_3$ 6	SiO_2 4	K_2O 8–12	MgO 6	$Mg(OH)_2$ 6	H_2O	CaO 6	CaO 8–*z*	Na_2O 6–8	FeO 6	$Fe(OH)_2$ 6	Fe_2O_3 6
1. Kaolinite	0.0	0.33	1.33	2.0	0.0	0.0	0.0	0.0	0.0	0.0	0.0	0.0	0.0	0.0
2. Muscovite	0.5	0.67	0.67	3.0	0.5	0.0	0.0	0.0	0.0	0.0	0.0	0.0	0.0	0.0
3. Margarite	1.0	0.67	0.67	2.0	0.0	0.0	0.0	0.0	1.0	0.0	0.0	0.0	0.0	0.0
4. Talc	0.0	0.0	0.0	4.0	0.0	2.0	1.0	0.0	0.0	0.0	0.0	0.0	0.0	0.0
5. Pyrophyllite	0.0	0.67	0.67	4.0	0.0	0.0	0.0	0.0	0.0	0.0	0.0	0.0	0.0	0.0
6. Microcline	0.5	0.0	0.0	3.0	0.5	0.0	0.0	0.0	0.0	0.0	0.0	0.0	0.0	0.0
7. Low albite	0.5	0.0	0.0	3.0	0.0	0.0	0.0	0.0	0.0	0.0	0.5	0.0	0.0	0.0
8. Anorthite	1.0	0.0	0.0	2.0	0.0	0.0	0.0	0.0	1.0	0.0	0.0	0.0	0.0	0.0
9. Analcime	0.5	0.0	0.0	2.0	0.0	0.0	0.0	1.0	0.0	0.0	0.5	0.0	0.0	0.0
10. Lawsonite	0.67	0.0	0.67	2.0	0.0	0.0	0.0	1.0	1.0	0.0	0.0	0.0	0.0	0.0
11. Ferrosilite	0.0	0.0	0.0	1.0	0.0	0.0	0.0	0.0	0.0	0.0	0.0	1.0	0.0	0.0
12. Fayalite	0.0	0.0	0.0	1.0	0.0	0.0	0.0	0.0	0.0	0.0	0.0	2.0	0.0	0.0
13. Leucite	0.5	0.0	0.0	2.0	0.5	0.0	0.0	0.0	0.0	0.0	0.0	0.0	0.0	0.0
14. Leonardite	1.0	0.0	0.0	4.0	0.0	0.0	0.0	3.5	0.0	1.0	0.0	0.0	0.0	0.0
15. Tremolite	0.0	0.0	0.0	4.0	0.0	2.0	0.5	0.0	0.0	1.0	0.0	0.0	0.0	0.0
16. Jadeite	0.0	0.5	0.0	2.0	0.0	0.0	0.0	0.0	0.0	0.0	0.5	0.0	0.0	0.0
17. Diopside	0.0	0.0	0.0	2.0	0.0	1.0	0.0	0.0	0.0	1.0	0.0	0.0	0.0	0.0
18. Merwinite	0.0	0.0	0.0	2.0	0.0	1.0	0.0	0.0	3.0	0.0	0.0	0.0	0.0	0.0
19. Monticellite	0.0	0.0	0.0	1.0	0.0	1.0	0.0	0.0	1.0	0.0	0.0	0.0	0.0	0.0
20. Grossular	0.0	1.0	0.0	3.0	0.0	0.0	0.0	0.0	0.0	3.0	0.0	0.0	0.0	0.0
21. Zoisite	0.0	1.33	0.33	3.0	0.0	0.0	0.0	0.0	0.0	2.0	0.0	0.0	0.0	0.0
22. Mordenite	0.47	0.0	0.0	5.06	0.0	0.0	0.0	3.47	0.0	0.29	0.18	0.0	0.0	0.0
23. Yugawaralite	0.5	0.0	0.0	3.0	0.0	0.0	0.0	2.0	0.0	0.5	0.0	0.0	0.0	0.0
24. Grunerite	0.0	0.0	0.0	4.0	0.0	0.0	0.0	0.0	0.0	0.0	0.0	3.0	0.5	0.0
25. Minnesotaite	0.0	0.0	0.0	4.0	0.0	0.0	0.0	0.0	0.0	0.0	0.0	2.0	1.0	0.0
26. Riebeckite	0.0	0.0	0.0	4.0	0.0	0.0	0.0	0.0	0.0	0.0	0.5	1.0	0.5	0.5
27. Chrysotile	0.0	0.0	0.0	2.0	0.0	1.0	2.0	0.0	0.0	0.0	0.0	0.0	0.0	0.0
28. Paragonite	0.5	0.67	0.67	3.0	0.0	0.0	0.0	0.0	0.0	0.0	0.5	0.0	0.0	0.0
29. Phlogopite	0.5	0.0	0.0	3.0	0.5	2.0	1.0	0.0	0.0	0.0	0.0	0.0	0.0	0.0
30. Laumontite	1.0	0.0	0.0	4.0	0.0	0.0	0.0	4.0	0.0	1.0	0.0	0.0	0.0	0.0
31. Nepheline	0.5	0.0	0.0	1.0	0.0	0.0	0.0	0.0	0.0	0.0	0.5	0.0	0.0	0.0
32. Greenalite	0.0	0.0	0.0	2.0	0.0	0.0	0.0	0.0	0.0	0.0	0.0	1.0	2.0	0.0
33. Prehnite	0.67	0.0	0.67	3.0	0.0	0.0	0.0	0.0	1.0	1.0	0.0	0.0	0.0	0.0
34. Acmite	0.0	0.0	0.0	2.0	0.0	0.0	0.0	0.0	0.0	0.0	0.5	0.0	0.0	0.5

Note: Minerals used in ΔG_f^0 model: 1–27, 33, 34. Minerals used in ΔH_f^0 model: 1–32.

of basic polyhedral units (Hazen, 1985). Using this polyhedral approach, volume, bulk modulus (Hazen, 1985), stable-isotope fractionation (Savin and Lee, 1988), and refractive index (Bloss et al., 1983) can be modeled accurately. In turn, it seems reasonable that the thermodynamic properties of minerals could be estimated by summing the contributions of the individual polyhedra. We have determined, by multiple linear regression, the contribution of $^{[4]}Al_2O_3$, $^{[6]}Al_2O_3$, $^{[6]}Al(OH)_3$, $^{[4]}SiO_2$, $^{[6]}MgO$, $^{[6]}Mg(OH)_2$, $^{[6]}CaO$, $^{[8-z]}CaO$, $^{[6-8]}Na_2O$, $^{[8-12]}K_2O$, H_2O, $^{[6]}FeO$, $^{[6]}Fe(OH)_2$, and $^{[6]}Fe_2O_3$ components to the total ΔG_f^0 and ΔH_f^0 of a selected group of silicate minerals, where the z in $^{[8-z]}CaO$ represents coordination of these CaO polyhedra in zeolite structures. We propose that the thermodynamic properties of many silicate phases that are too complex and too impure to give reliable calorimetric measurements can be estimated by summing the contributions of these components for the mineral of interest.

This approach has many advantages over other estimation techniques. First, thermodynamic properties of the minerals used to calibrate the model are based on calorimetric and high-temperature phase-equilibrium measurements rather than on harder-to-determine solubility measurements. Second, it is conceptually simple and compelling to analyze a silicate mineral's properties in terms of the contributions of its "building block" oxide and/or hydroxide. Third, this technique is simple to implement because only the chemical formula and the coordination number of the polyhedra composing the mineral are needed. Finally, because of the large body of data available for use in the regression model, small errors in individual measurements have little effect on the estimated coefficients.

METHODS

A critically selected thermodynamic data base for 34 minerals was used (Table 1). The "building block" components for each mineral and the associated coordination numbers in the $^{[4]}Al_2O_3$-$^{[6]}Al_2O_3$-$^{[6]}Al(OH)_3$-$^{[4]}SiO_2$-$^{[6]}MgO$-$^{[6]}Mg(OH)_2$-$^{[6]}CaO$-$^{[8-z]}CaO$-$^{[6-8]}Na_2O$-$^{[8-12]}K_2O$-H_2O-$^{[6]}FeO$-$^{[6]}Fe(OH)_2$-$^{[6]}Fe_2O_3$ system were determined (Table 1). For example, the mineral kaolinite $[Al_2Si_2O_5(OH)_4]$ is composed of 2 $^{[4]}SiO_2$, 0.667 $^{[6]}Al_2O_3$, and 0.667 $^{[6]}Al(OH)_3$ polyhedra. When Al^{3+}, Fe^{3+}, Mg^{2+}, and Fe^{2+} are in sixfold coordination in the octahedral sheet of 1:1 and 2:1 phyllosilicate minerals, they were distributed as 0.6666 hydroxide and 0.3333 oxide, and 0.3333 hydroxide and 0.6666 oxide, respectively. This distribution is consistent with structural constraints on the distribution of oxide and hydroxide polyhedra (Weaver and Pollard, 1973). The number of $^{[4]}SiO_2$ polyhedra for an individual mineral in the regression model was not allowed to exceed

TABLE 2. The g_i and h_i of each polyhedral type

Polyhedral unit	g_i (kJ·mol^{-1})	Error (kJ·mol^{-1})	h_i (kJ·mol^{-1})	Error* (kJ·mol^{-1})
$^{[4]}Al_2O_3$	−1631.32	13.3	−1716.24	11.0
$^{[6]}Al_2O_3$	−1594.52	15.3	−1690.18	15.9
$^{[6]}Al(OH)_3$	−1181.62	13.2	−1319.55	12.2
$^{[4]}SiO_2$	−853.95	4.6	−910.97	3.2
$^{[6]}MgO$	−628.86	10.6	−660.06	7.9
$^{[6]}Mg(OH)_2$	−851.86	10.2	−941.62	9.1
$^{[6]}CaO$	−669.13	5.9	−696.65	5.2
$^{[6-7]}CaO$	−710.08	7.2	−736.04	7.1
$^{[6-8]}Na_2O$	−672.50	26.0	−683.00	18.4
$^{[8-12]}K_2O$	−722.94	27.4	−735.24	21.1
H_2O	−239.91	5.7	−292.37	4.6
$^{[6]}FeO$	−266.29	6.8	−290.55	5.4
$^{[6]}Fe(OH)_2$	−542.04	24.6	−596.07	8.2
$^{[6]}Fe_2O_3$	−776.07	33.0	−939.18	35.6

* Standard error of the estimate.

5.0 to avoid over-weighting the contribution of a particular mineral. If the sum of the associated $^{[4]}SiO_2$ polyhedra totaled more than five, one-half of the chemical formula was used. The rationale of this breakdown process was aided by a discussion of coordination numbers in silicates presented in Robinson and Haas (1983). A tabulation of the polyhedral coordination of oxide components of many silicate minerals is given by Smyth and Bish (1988).

The data were regressed to determine g_i and h_i (the contribution of 1 mol of component to the free energy and enthalpy of the mineral, respectively) for the following models: $\Delta G_f^0 = \Sigma\, n_i g_i$ (29 minerals) and $\Delta H_f^0 = \Sigma\, n_i h_i$ (32 minerals), where n_i is the number of moles of component i. Entropy values (S^0) can be determined using the equation $\Delta G_f^0 = \Delta H_f^0 - T\Delta S_f^0$, where $\Delta S_f^0 = S^0_{\text{elements}} - S^0$. S^0 estimations from both a regression model $S^0 = \Sigma\, n_i s_i$ (25 minerals) and from the above equation were found to have much larger associated errors and to be more sensitive to the coordination than enthalpy and free-energy values. We suggest using these techniques only for rough estimates of S^0. The technique of Holland (1989) gives more accurate estimates of S^0 and can be used in conjunction with our ΔH_f^0 model to produce an internally consistent set of ΔG_f^0, ΔH_f^0, and S^0 values.

A few minerals showed poor agreement between measured and predicted values. Beware of minerals such as pyrope, akermanite, and wollastonite that have oxides with unusual coordination numbers because data for polyhedra with these coordination numbers are not specified by the model. Other minerals that resulted in poor fits to the model include Ca-Al pyroxene, forsterite, cordierite, andradite, and gehlenite. We have no explanation for their inconsistency.

RESULTS

Table 2 lists g_i and h_i and their errors derived from the model. Tables 3 and 4 show measured ΔG_f^0 and ΔH_f^0 versus those predicted using g_i and h_i from Table 2. The average difference between the predicted and the measured values is 0.26% for ΔG_f^0 and 0.24% for ΔH_f^0, and these differences are normally distributed. The average reported associated errors (2σ) for the experimentally determined thermodynamic values are 0.16% for ΔG_f^0 and 0.13% for ΔH_f^0. Approximately 50% of the estimated values fall within the range of the error (2σ) reported for the experimentally determined data.

TABLE 3. Comparison of ΔG_f^0 (measured) versus ΔG_f^0 (predicted) for the 29 minerals used in the model and the associated errors

Mineral	ΔG_f^0 (measured) (kJ·mol^{-1})	ΔG_f^0 (predicted) (kJ·mol^{-1})	Residuals (kJ·mol^{-1})	% Residual
1. Kaolinite	−3799.4	−3814.9	15.5	0.41
2. Muscovite	−5595.5	−5589.7	−5.8	0.10
3. Margarite	−5854.8	−5859.1	4.3	0.07
4. Talc	−5536.1	−5525.4	−10.7	0.19
5. Pyrophyllite	−5265.9	−5266.6	0.6	0.01
6. Microcline	−3742.3	−3739.0	−3.4	0.09
7. Low albite	−3711.7	−3713.8	2.0	0.05
8. Anorthite	−4002.1	−4008.3	6.3	0.16
9. Analcime	−3091.7	−3099.7	8.0	0.26
10. Lawsonite	−4525.6	−4492.2	−33.4	0.74
11. Ferrosilite	−1117.1	−1120.2	−3.1	0.28
12. Fayalite	−1379.4	−1386.5	−7.2	0.52
13. Leucite	−2875.9	−2885.0	9.1	0.32
14. Leonardite	−6598.6	−6596.9	−1.7	0.03
15. Tremolite	−5814.0	−5809.5	−4.4	0.08
16. Jadeite	−2850.8	−2841.4	−9.4	0.33
17. Diopside	−3036.6	−3046.8	10.3	0.34
18. Merwinite	−4339.4	−4344.1	4.7	0.11
19. Monticellite	−2143.2	−2151.9	8.8	0.41
20. Grossular	−6295.3	−6286.6	−8.7	0.14
21. Zoisite	−6495.3	−6501.9	6.6	0.10
22. Mordenite	−6247.6	−6246.0	−1.6	0.03
23. Yugawaralite	−4193.9	−4212.4	18.5	0.44
24. Grunerite	−4494.4	−4485.7	−8.7	0.19
25. Minnesotaite	−4474.8	−4490.4	15.6	0.35
26. Chrysotile	−4034.0	−4040.5	6.5	0.16
27. Prehnite	−5816.4	−5816.3	−0.1	0.00
28. Riebeckite	−4699.9	−4677.4	−22.5	0.48
29. Acmite	−2409.7	−2432.2	22.5	0.93
Average				0.26

Note: 1, 4, 6, 7, 8, 9, 10, 12, 13, 14, 15, 16, 17, 18, 19, and 26—Robie et al. (1978). 2, 5, and 20—Krupka et al. (1979). 3, 21, and 27—Hemingway et al. (1982). 22—Johnson et al. (1986). These data were determined by calorimetry.

23—Zeng and Liou (1982). 11, 24, and 25—Miyano and Klein (1983). 28 and 29—Makarov et al. (1984). These data were determined from phase-equilibrium reversals.

The accuracy of the models was tested by predicting the thermodynamic properties of minerals not used to develop the model. Table 5a compares the results of the model with calorimetrically determined thermodynamic data for 20 different minerals and gives associated differences. Average residuals for these minerals are 0.25% for ΔG_f^0 for 18 minerals and 0.22% for ΔH_f^0 for 20 minerals. Table 5b shows that ΔG_f^0 values derived from solubility measurements of clays agree with those predicted by this model with an average difference of 0.54% between the predicted and measured ΔG_f^0 for 18 minerals.

DISCUSSION

A comparison of the g_i and h_i from these models to the ΔG_f^0 and ΔH_f^0 for the simple oxide or hydroxide compo-

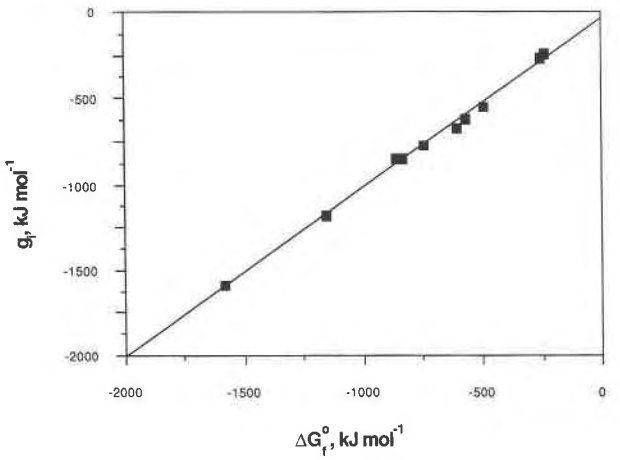

Fig. 1. Graph of the g_i (kJ·mol^{-1}) versus $\Delta G^\circ_{f,ox.\text{-}hyd.}$ (kJ·mol^{-1}) data from Table 6. The associated regression equation is $g_i = -35.55 + 0.990\Delta G^\circ_{f,ox.\text{-}hyd.}$ with an R value equal to 1.00.

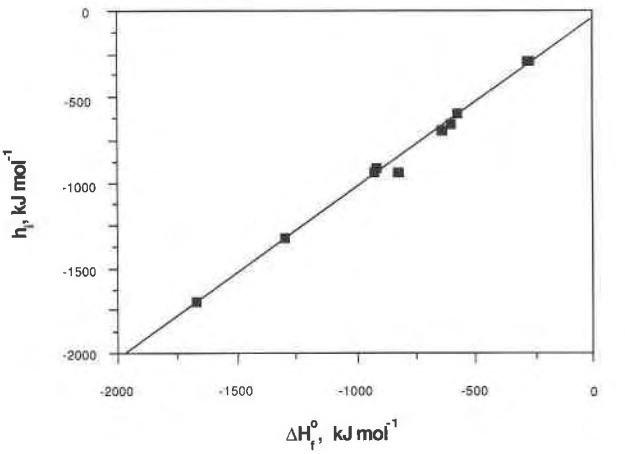

Fig. 2. Graph of the h_i (kJ·mol^{-1}) versus $\Delta H^\circ_{f,ox.\text{-}hyd.}$ (kJ·mol^{-1}) data from Table 6. The associated regression equation is $h_i = -38.29 + 0.995\Delta H^\circ_{f,ox.\text{-}hyd.}$ with an R value equal to 1.00.

TABLE 4. Comparison of ΔH_f° *(measured)* versus ΔH_f° *(predicted)* for the 32 minerals used in the model and the associated errors

Mineral	ΔH_f° (measured) (kJ·mol^{-1})	ΔH_f° (predicted) (kJ·mol^{-1})	Residual (kJ·mol^{-1})	% Residual
1. Kaolinite	−4133.6	−4144.7	11.1	0.27
2. Muscovite	−5971.6	−5965.1	−6.5	0.11
3. Paragonite	−5941.5	−5939.0	−2.5	0.04
4. Margarite	−6239.6	−6241.3	1.7	0.03
5. Phlogopite	−6213.9	−6220.4	6.5	0.10
6. Talc	−5915.9	−5905.6	−10.3	0.17
7. Pyrophyllite	−5639.8	−5650.4	10.6	0.18
8. Microcline	−3967.7	−3958.7	−9.0	0.22
9. Low albite	−3935.1	−3932.5	−2.6	0.07
10. Anorthite	−4227.8	−4234.8	7.0	0.16
11. Analcime	−3309.8	−3313.9	4.1	0.12
12. Laumontite	−7277.2	−7265.6	−11.5	0.16
13. Lawsonite	−4863.9	−4834.8	−29.1	0.60
14. Ferrosilite	−1194.9	−1201.5	6.7	0.56
15. Fayalite	−1479.4	−1492.1	12.7	0.86
16. Leucite	−3038.7	−3047.7	9.0	0.30
17. Nepheline	−2092.1	−2110.6	18.5	0.88
18. Leonardite	−7123.2	−7119.4	−3.8	0.05
19. Tremolite	−6177.5	−6170.9	−6.7	0.11
20. Jadeite	−3029.4	−3008.5	−20.9	0.69
21. Diopside	−3210.8	−3218.0	7.3	0.23
22. Merwinite	−4566.8	−4571.9	5.2	0.11
23. Monticellite	−2262.7	−2267.7	5.0	0.22
24. Grossular	−6636.3	−6631.2	−5.1	0.08
25. Zoisite	−6891.1	−6898.4	7.3	0.10
26. Mordenite	−6756.2	−6765.7	9.5	0.14
27. Yugawaralite	−4518.1	−4543.8	25.7	0.57
28. Grunerite	−4824.2	−4813.6	−10.6	0.22
29. Minnesotaite	−4823.0	−4821.0	−2.0	0.04
30. Chrysotile	−4361.7	−4365.2	3.6	0.08
31. Greenalite	−3301.0	−3304.6	3.6	0.10
32. Riebeckite	−5043.6	−5043.6	0.0	0.00
Average				0.24

Note: 2, 7, 13, and 24—Krupka et al. (1979). 4 and 25—Hemingway et al. (1982). 5—Clemens et al. (1987). 6, 8, 9, 10, 11, 15, 16, 17, 18, 19, 20, 21, 22, 23, and 30—Robie et al. (1978). 26—Johnson et al. (1986). These data were determined by calorimetry.

1—Hemley et al. (1980). 3 and 12—Berman et al. (1985). 27—Zeng and Liou (1982). 14, 28, 29, and 31—Miyano and Klein (1983). 32—Makarov et al. (1984). These data were determined from phase-equilibrium reversals.

nents (Table 6) shows that there is a good correlation between g_i and ΔG_f° (Fig. 1) and between h_i and ΔH_f° (Fig. 2). These graphs show that free energy and enthalpy of formation of an oxide or hydroxide component in a silicate mineral generally is more negative than those of the simple oxide or hydroxide mineral by ~36 kJ·mol^{-1} and ~38 kJ·mol^{-1}, respectively. The abundance of silicate minerals relative to free oxides and hydroxides in nature is consistent with this relationship.

The correlation lines in Figures 1 and 2 can be used to approximate a g_i or h_i for polyhedra not determined by this model. For example, experimental data for a mineral containing a $Fe(OH)_3$ polyhedron was not available to incorporate into these models, but g_i and h_i can be approximated by using the experimentally determined $\Delta G_f^\circ[Fe(OH)_3]$ and $\Delta H_f^\circ[Fe(OH)_3]$. The values of $\Delta G_f^\circ = -696.50$ kJ·mol^{-1} and $\Delta H_f^\circ = -823.0$ kJ·mol^{-1} (Wagman et al., 1982) can be used along with $g_i = -35.6 + 0.990\Delta G_f^\circ$ and $h_i = -38.3 + 0.995\Delta H_f^\circ$ to estimate $g_i = -725.0$ kJ·mol^{-1}, and $h_i = -856.8$ kJ·mol^{-1}. However, the errors associated with these estimates are unknown and may be large.

Table 7 describes the protocol to follow when estimating the thermodynamic properties of a silicate mineral using the model described above. It shows, as an example, the estimation of ΔG_f° for an illite $[K_{0.75}(Al_{1.75}Mg_{0.25})Si_{3.5}Al_{0.5}O_{10}(OH)_2]$. The estimated ΔG_f° of this illite is −5463.0 kJ·mol^{-1}. Using an analogous procedure, it was found that $\Delta H_f^\circ = -5837.3$ kJ·mol^{-1}. Note that the procedure for distributing the octahedral cations in step 2b is based on crystallographic constraints (Weaver and Pollard, 1973). On the other hand, the distribution of cations into the interlayer of chlorites (step 2c) is based on a thermodynamic argument, which results in the most negative (stable) ΔG_f° for a given composition. Also, using $\Delta G^\circ_{f,ox.\text{-}hyd.}$ and $\Delta H^\circ_{f,ox.\text{-}hyd.}$ for cations in the chlorite interlayer is justified by the fact that chlorite interlayers act as

TABLE 5A. Measured ΔG_f° and ΔH_f° determined by calorimetry compared to their predicted values for 20 minerals

Mineral (Ref.)*	Chemical formula	ΔG_f° (pred.) (kJ·mol^{-1})	ΔG_f° (meas.) (kJ·mol^{-1})	% Difference	ΔH_f° (pred.) (kJ·mol^{-1})	ΔH_f° (meas.) (kJ·mol^{-1})	% Difference
Nepheline (1)	$Na_{0.78}K_{0.22}AlSiO_4$	−2011.4	—	—	−2116.3	−2110.3	0.28
Mesolite (2)	$Na_{0.676}Ca_{0.657}Al_{1.990}Si_{3.01}O_{10}\cdot 2.647H_2O$	−5530.6	−5513.2	0.32	−5946.6	−5947.1	0.01
Natrolite (2)	$Na_2Al_2Si_3O_{10}\cdot 2.0H_2O$	−5345.5	−5316.6	0.54	−5716.9	−5718.6	0.03
Scolecite (2)	$CaAl_2Si_3O_{10}\cdot 3.0H_2O$	−5623.0	−5597.9	0.45	−6062.3	−6049.0	0.22
Stilbite (3)	$Na_{0.136}Ca_{1.02}K_{0.006}Al_{2.180}Si_{6.820}O_{18}\cdot 7.33H_2O$	−10132.1	−10143.0	0.11	−11025.2	−11034.6	0.09
Ca-olivine (4)	Ca_2SiO_4	−2192.2	−2199.7	0.34	−2304.3	−2316.5	0.53
Kyanite (4)	Al_2SiO_5	−2448.5	−2444.0	0.18	−2601.2	−2594.3	0.26
Prehnite (4)	$Ca_2Al_2Si_3O_{10}(OH)_2$	***	−5816.4	***	−6189.5	−6193.6	0.07
Hedenbergite (5)	$CaFeSi_2O_6$	−2684.3	−2674.3	0.37	−2848.5	−2837.6	0.38
Almandine (6)	$Fe_3Al_2Si_3O_{12}$	−4955.2	−4951.3	0.08	−5294.7	−5275.5	0.36
Oligoclase (7)	$Ca_{0.2}Na_{0.8}Al_{1.2}Si_{2.8}O_8$	−3772.7	−3754.3	0.49	−3993.0	−3977.3	0.39
Andesine (7)	$Ca_{0.4}Na_{0.6}Al_{1.4}Si_{2.6}O_8$	−3831.6	−3818.3	0.35	−4053.5	−4041.7	0.29
Labradorite (7)	$Ca_{0.5}Na_{0.5}Al_{1.5}Si_{2.5}O_8$	−3861.1	−3848.9	0.32	−4083.7	−4072.3	0.28
Bytownite (7)	$Ca_{0.8}Na_{0.2}Al_{1.8}Si_{2.2}O_8$	−3949.4	−3959.7	0.26	−4174.4	−4184.0	0.23
Merlionite (8)	$KAlSi_{1.94}O_{5.88}\cdot 1.69H_2O$	−3239.2	−3241.4	0.07	−3487.1	−3481.8	0.15
Merlionite (8)	$KAlSi_{1.81}O_{5.62}\cdot 1.69H_2O$	−3128.2	−3123.3	0.16	−3368.7	−3359.9	0.26
Merlionite (8)	$K_{0.80}Na_{0.20}AlSi_{1.94}O_{5.88}\cdot 1.81H_2O$	−3263.0	−3272.2	0.28	−3517.0	−3519.0	0.06
Merlionite (8)	$K_{0.91}Na_{0.09}AlSi_{1.81}O_{5.62}\cdot 1.79H_2O$	−3150.0	−3144.6	0.17	−3395.6	−3387.3	0.25
Merlionite (8)	$Na_{0.81}K_{0.19}AlSi_{1.94}O_{5.88}\cdot 2.13H_2O$	−3324.4	−3325.8	0.04	−3594.6	−3591.2	0.10
Merlionite (8)	$Na_{0.81}K_{0.19}AlSi_{1.81}O_{5.62}\cdot 2.18H_2O$	−3225.4	−3225.3	0.00	−3490.8	−3488.3	0.07
Average				0.25			0.22

Note: — = not determined. *** = value used in the model.

* References: (1) Robie et al. (1978). (2) Johnson et al. (1983). (3) O'Hare et al. (1986). (4) Hemingway et al. (1982). (5) Robie et al. (1987). (6) Chaterjee (1987). (7) Naumov et al. (1974). (8) Donahoe et al. (1990a, 1990b).

simple oxide-hydroxide phases rather than as part of the silicate lattice. The presence of $Fe(OH)_2$ and $Mg(OH)_2$ in chlorite interlayers will be proposed later in this paper as a buffer to control the Fe^{2+} and Mg^{2+} contents of natural waters.

The difference between the thermodynamic properties of the oxide or hydroxide components in silicate minerals (g_i and h_i) and those components in simple minerals (ΔG_f° and ΔH_f°) is primarily a result of each interaction of the polyhedron with its nearest neighbors. For example, $Al(OH)_3$ in gibbsite is surrounded by six $Al(OH)_3$ polyhedra, whereas an $Al(OH)_3$ polyhedron in the silicate

TABLE 5B. ΔG_f° determined from solubility measurements compared to predicted ΔG_f° for 18 minerals along with the ΔH_f° predicted by the model

Mineral (Ref.)*	Chemical formula	ΔG_f° (pred.) (kJ·mol^{-1})	ΔG_f° (meas.) (kJ·mol^{-1})	% Difference	ΔH_f° (pred.) (kJ·mol^{-1})
Kerolite (9)	$Mg_3Si_4O_{10}(OH)_2\cdot H_2O$	−5765.3	−5828.03	1.07	−6198.0
Sepiolite (9)	$Mg_2Si_3O_{7.5}(OH)\cdot 3H_2O$	−4650.8	−4692.80	0.89	−5070.9
Chlorite 1 (10)	$(Al_{1.44}Fe^{3+}_{0.07}Fe^{2+}_{0.99}Mg_{3.24})Al_{1.03}Si_{2.97}O_{10}(OH)_8$	−7819.8	−7793.00	0.34	−8477.2
Chlorite 2 (10)	$(Al_{1.75}Fe^{3+}_{0.12}Fe^{2+}_{2.61}Mg_{1.16})Al_{1.16}Si_{2.84}O_{10}(OH)_8$	−7321.5	−7319.00	0.03	−7952.3
Chlorite 3 (10)	$(Al_{1.60}Fe^{3+}_{3.29}Mg_{1.05})Al_{1.53}Si_{2.47}O_{10}(OH)_8$	−7282.0	−7290.00	0.11	−7932.6
Chlorite 4 (10)	$(Al_{1.39}Fe^{3+}_{0.21}Fe^{2+}_{0.57}Mg_{3.52})Al_{1.01}Si_{2.99}O_{10}(OH)_8$	−7888.2	−7869.00	0.24	−8553.5
Fithian illite (11)	$K_{0.64}(Al_{1.54}Fe^{3+}_{0.29}Mg_{0.19})Al_{0.49}Si_{3.51}O_{10}(OH)_2$	−5329.6	−5443.40	2.09	−5715.0
Great Lake illite (11)	$K_{0.59}(Al_{1.58}Fe^{3+}_{0.24}Mg_{0.15})Al_{0.35}Si_{3.65}O_{10}(OH)_2$	−5299.2	−5345.90	0.87	−5683.0
Big Bend illite (11)	$K_{0.60}Na_{0.04}(Al_{1.43}Fe^{3+}_{0.42}Mg_{0.16})Al_{0.52}Si_{3.48}O_{10}(OH)_2$	−5268.5	−5333.34	1.21	−5656.5
Clay Spur (12)	$K_{0.02}Ca_{0.1}Na_{0.27}(Al_{1.52}Fe^{3+}_{0.19}Mg_{0.22})Al_{0.08}Si_{3.94}O_{10}(OH)_2$	−5227.6	−5226.40	0.02	−5612.8
Cheto (12)	$K_{0.02}Ca_{0.185}Na_{0.02}(Al_{1.52}Fe^{3+}_{0.14}Mg_{0.33})Al_{0.07}Si_{3.93}O_{10}(OH)_2$	−5251.8	−5245.30	0.12	−5639.4
K-Beidellite (13)	$K_{0.37}Ca_{0.01}Na_{0.07}(Al_{1.41}Fe^{3+}_{0.415}Fe^{2+}_{0.055}Mg_{0.205})Al_{0.45}Si_{3.55}O_{10}(OH)_2$	−5234.5	−5215.40	0.36	−5625.5
Mg-Beidellite (13)	$K_{0.095}Ca_{0.01}Na_{0.07}Mg_{0.135}(Al_{1.41}Fe^{3+}_{0.415}Fe^{2+}_{0.055}Mg_{0.205})$-$Al_{0.45}Si_{3.55}O_{10}(OH)_2$	−5219.3	−5200.10	0.37	−5614.1
Smectite (14)	$Mg_{0.225}(Al_{1.345}Fe^{3+}_{0.405}Mg_{0.27})Al_{0.30}Si_{3.70}O_{10}(OH)_2$	−5174.2	−5214.70	0.78	−5568.5
Al: Belle Fouche (15)	$Al_{0.0883}(Al_{1.515}Fe^{3+}_{0.225}Mg_{0.29})Al_{0.065}Si_{3.935}O_{10}(OH)_2$	−5193.9	−5213.40	0.37	−5587.3
Mg: Belle Fouche (15)	$Mg_{0.1325}(Al_{1.515}Fe^{3+}_{0.225}Mg_{0.29})Al_{0.065}Si_{3.935}O_{10}(OH)_2$	−5207.4	−5222.80	0.29	−5600.1
Al: Aberdeen (15)	$Al_{0.1383}(Al_{1.29}Fe^{3+}_{0.335}Mg_{0.445})Al_{0.18}Si_{3.82}O_{10}(OH)_2$	−5185.8	−5200.00	0.27	−5581.0
Mg: Aberdeen (15)	$Mg_{0.2075}(Al_{1.29}Fe^{3+}_{0.335}Mg_{0.445})Al_{0.18}Si_{3.82}O_{10}(OH)_2$	−5206.9	−5218.70	0.23	−5601.0
Average				0.54	

* References: 9—Stoessel (1988). 10—Kittrick (1982). 11—Kittrick (1984). 12—Huang and Keller (1973). 13—Misra and Upchurch (1976). 14—Carson et al. (1976). 15—Kittrick (1971a, 1971b, 1971c).

TABLE 6. ΔG_f^0 and ΔH_f^0 of the free oxide or hydroxide phases compared to g_i and h_i from the multiple linear-regression model

Oxide or hydroxide	$\Delta G^0_{f,ox\text{-}hyd.}$ (kJ·mol^{-1})	g_i (kJ·mol^{-1})	$\Delta H^0_{f,ox\text{-}hyd.}$ (kJ·mol^{-1})	h_i (kJ·mol^{-1})
$^{[6]}Al_2O_3$	−1582.23	−1594.52	−1675.70	−1690.18
$Al(OH)_3$	−1154.89	−1181.62	−1293.13	−1319.55
SiO_2	−856.29	−853.95	−910.70	−910.97
MgO	−569.20	−628.86	−601.49	−660.06
$Mg(OH)_2$	−833.51	−851.86	−924.54	−941.62
H_2O	−237.14	−239.91	−285.83	−292.37
$^{[6]}CaO$	−603.49	−669.13	−635.09	−696.65
FeO	−251.16	−266.29	−272.04	−290.55
Fe_2O_3	−742.68	−776.07	−824.64	−939.18
$Fe(OH)_2$	−492.04	−542.04	−574.04	−596.07

Note: All measured thermodynamic data from Robie et al. (1978), except for $Fe(OH)_2$, which is from Nordstrom et al. (1984).

TABLE 7. Method of estimation of ΔG_f^0 and ΔH_f^0 (in kJ·mol^{-1}) for a mineral

1. Determine chemical composition (analytical electron microscopy, microprobe, X-ray fluorescence, or wet-chemical analysis).
2. Determine coordination based on known structures.
   A. For Ca-bearing zeolite minerals with an unknown coordination number, the polyhedra is simply represented with a "*z*."
   B. For 1:1 phyllosilicate minerals, distribute the octahedral cations as 0.6666 hydroxide and 0.3333 oxide. For 2:1 phyllosilicate minerals, the octahedral cations are distributed as 0.3333 hydroxide and 0.6666 oxide.
   C. For chlorites, distribute cations into the interlayer in the order $Al^{3+} > Fe^{2+} \geq Mg^{2+} > Fe^{3+}$ until the $(OH)_{interlayer\ total} = 8$. The remaining cations are then distributed into the octahedral sheet following the method in 2B.
3. Determine the number of polyhedra, *n*, of each component in the formula unit.
4. Multiply *n* by the g_i and h_i values (Table 2). The interlayer thermodynamic contribution for chlorites is then calculated by multiplying ΔG_f^0 and ΔH_f^0 of free oxide or hydroxide (Table 6) by the corresponding values of *n* determined in 2C.
5. Calculate ΔG_f^0 and ΔH_f^0 for the mineral of interest by summing the polyhedral contributions.

Example: Estimation of the ΔG_f^0 of an illite

1. Chemical formula = $K_{0.75}(Al_{1.75}Mg_{0.25})Si_{3.5}Al_{0.50}O_{10}(OH)_2$
2. In this structure the polyhedra are $^{[4]}Al_2O_3$, $^{[6]}Al_2O_3$, $^{[6]}Al(OH)_3$, $^{[4]}SiO_2$, $^{[6]}MgO$, $^{[6]}Mg(OH)_2$, and $^{[8-12]}K_2O$.
3. The number of each polyhedra are $0.2500^{[4]}Al_2O_3$, $0.5833^{[6]}Al_2O_3$, $0.5833^{[6]}Al(OH)_3$, $3.500^{[4]}SiO_2$, $0.1666^{[6]}MgO$, $0.08333^{[6]}Mg(OH)_2$, and $0.3750^{[8-12]}K_2O$.
4. $\Delta G_f^0 = 0.2500g_f^{[4]}Al_2O_3 + 0.5833g_f^{[6]}Al_2O_3 + 0.5833g_f^{[6]}Al(OH)_3 + 3.500g_f^{[4]}SiO_2 + 0.1666g_f^{[6]}MgO + 0.08333g_f^{[6]}Mg(OH)_2 + 0.3750g_f^{[8-12]}K_2O$.
   $\Delta G_f^0 = [(0.2500)(-1631.32) + (0.5833)(-1594.52) + (0.5833)(-1181.62) + (3.500)(-853.95) + (0.1666)(-628.86) + (0.08333)(-851.86) + (0.3750)(-722.94)]$.
5. $\Delta G_f^0 = -5463.0$ kJ·mol^{-1}; ΔH_f^0 can be determined the same way.

minerals considered in this model is generally surrounded by, at most, only two $Al(OH)_3$ polyhedra with the other sites occupied by other tetrahedral components (generally SiO_2). The presence of these other components in the nearest-neighbor sites clearly stabilizes the $Al(OH)_3$ in the silicates by the amount $g_i - \Delta G_f^0 \approx 28$ kJ·mol^{-1}. The amount of this stabilization varies from site to site depending on the composition of the nearest-neighbor shell, but the efficacy of the model presented here demonstrates that this stabilization value is fairly constant for a wide variety of sites in a wide range of silicate compositions, regardless of structure type. Conversely, however, this consideration means that the coefficients derived in this model are likely to be useful only for silicates. Notice that in Table 6 the only polyhedron in which $g_i > \Delta G_f^0$ is SiO_2; this is consistent with quartz's being a very common mineral.

Thermodynamic data for ordered phases were chosen, whenever available, to create this model. As a result it seems likely that the estimated ΔG_f^0 and ΔH_f^0 values should be closest to those for a completely ordered mineral. Please note, however, that the variation in these values between ordered and disordered phases is generally smaller than the uncertainty of the estimate. For example, the differences between ΔG_f^0 and ΔH_f^0 for microcline versus sanidine is 0.07% and 0.20%, respectively (Robie et al., 1978), whereas the uncertainty of our estimate of these values for microcline are on the order ±0.25%. A more sophisticated model will be necessary to develop enough resolution to account for order-disorder effects on these thermodynamic quantities.

This technique has a wide variety of applications in predicting thermodynamic properties of common zeolites and clays. First, the relative stability of clays in the K_2O-Al_2O_3-SiO_2-H_2O system will be discussed. Using the thermodynamic data in Table 8 a log a_{K^+}/a_{K^+} versus log $a_{H_4SiO_4}$ diagram at 298 K was constructed (Fig. 3). Figure 3 shows the metastability of Al-montmorillonite and Al-illite, which agrees with the 298-K experimental data of Sass et al. (1987). In order to represent natural compositions more closely, we determined the effect on ΔG_f^0 of the substitution of various cations (Fe^{3+}, Fe^{2+}, and Mg^{2+}) into the montmorillonite and illite structures (Table 8). Figure 3 shows how these cation substitutions shift the kaolinite-montmorillonite-illite triple point. Notice that the Fe^{3+} substitution seems to cause the greatest degree of stabilization of montmorillonite and illite. When writing reactions containing Fe^{3+}, Fe^{2+}, and Mg^{2+}, the concentrations of these cations in solution were assumed to be controlled by FeOOH, $Fe(OH)_2$, and $Mg(OH)_2$ solubilities. The choice of $Fe(OH)_2$ and $Mg(OH)_2$ as controls of Fe^{2+} and Mg^{2+} concentrations assumes the presence of chlorite interlayers containing these components, as previously discussed. If an amorphous ferric hydroxide phase controls the Fe^{3+} concentration, the kaolinite-montmorillonite-illite triple point becomes even more stable relative to kaolinite, microcline, and pyrophyllite.

This technique was also used to estimate the ΔG_f^0 of three K-zeolites: clinoptilolite, erionite, and phillipsite (Table 8). The results show that phillipsite is stable at SiO_2 concentrations of <12 ppm; erionite, between 12 and 16 ppm; and clinoptilolite, >16 ppm (Fig. 4). Extensive zeolite formation (clinoptilolite, erionite, and phillipsite) at surface conditions (25 °C) has been observed in

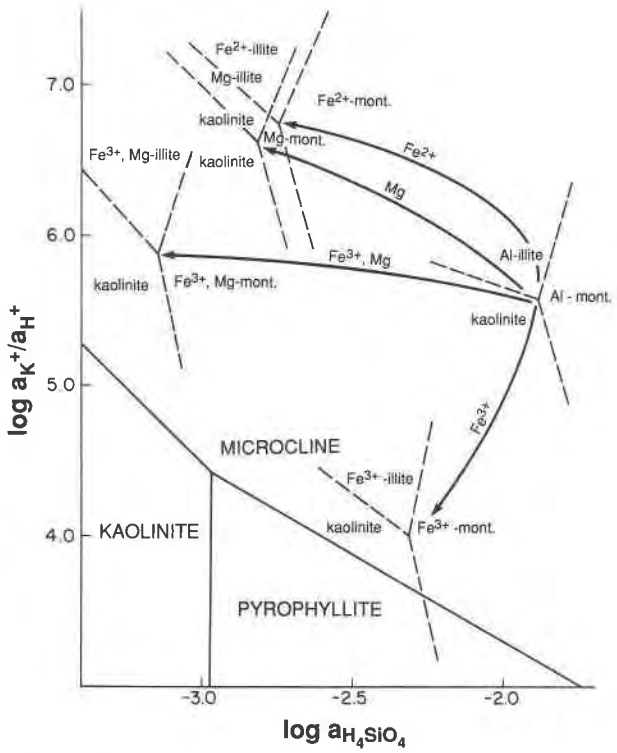

Fig. 3. Activity-activity diagram of the K_2O-Al_2O_3-SiO_2-H_2O system at 298 K showing the stable microcline-kaolinite-pyrophyllite triple point. This diagram also shows the effect of Mg^{2+}, Fe^{3+}, Fe^{2+}, and both Mg^{2+}-Fe^{3+} substitution (arrows) on the stability of the kaolinite-montmorillonite-illite triple point. Chemical compositions and thermodynamic data are given in Table 8.

altered volcanic tuffs (Hay, 1986; Sheppard and Gude, 1973). Senkayi et al. (1987) observed the coexistence of opal-CT–kaolinite–clinoptilolite at high silica concentrations, and Iijima (1978) reported that clinoptilolite and phillipsite are prominent in sediments in coexistence with interstitial water that has SiO_2 concentrations of between 6–42 ppm and 5–21 ppm, respectively. The constructed activity diagram (Fig. 4) is consistent with these natural observations.

Conclusions

The multiple linear-regression technique presented here is a simple and effective way to estimate the ΔG_f^0 and ΔH_f^0 of silicate minerals. The only data needed for this estimation technique are the chemical composition and the coordination of the "building block" polyhedra in the mineral of interest. The advantages of the technique include its simplicity (it can be programmed into a microcomputer spreadsheet program), the fact that the model is based on calorimetric and high-temperature phase-equilibrium measurements rather than more-difficult-to-perform solubility measurements, and its ability to model a wide range of silicate minerals. The technique gives results that agree quite well with a wide range of calorimetric and solubility data not used to derive the reported coefficients.

Although this technique seems to give reliable results for most cases, it should be used with some caution. We already know that the model presented here fails to predict accurately the thermodynamic properties of Ca-Al pyroxene, forsterite, cordierite, andradite, and gehlenite. There is no question that experimentally determined

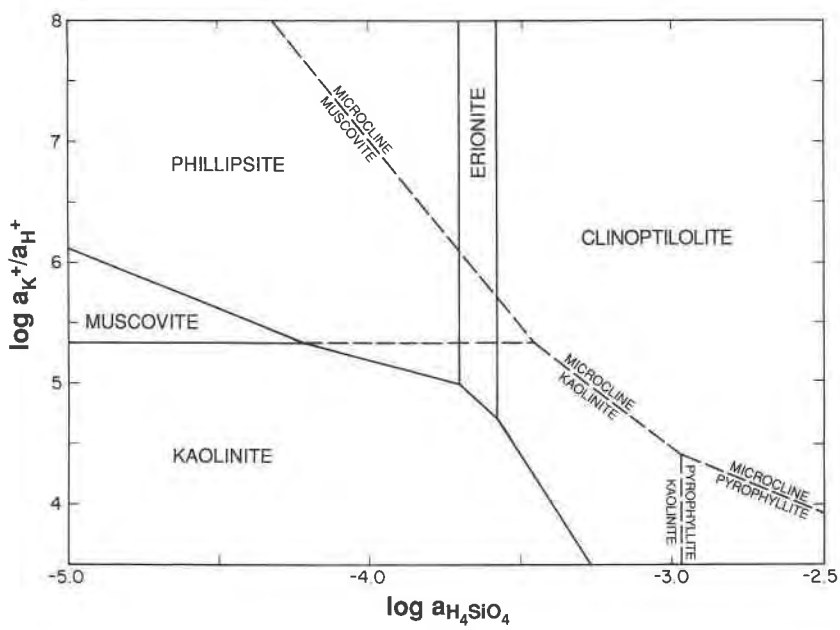

Fig. 4. Activity-activity diagram of the K_2O-Al_2O_3-SiO_2-H_2O system at 298 K showing three K-zeolite phases (phillipsite, erionite, and clinoptilolite). Thermodynamic data taken from Table 8.

TABLE 8. ΔG_f^0 data used in the calculation of K_2O-Al_2O_3-SiO_2-H_2O diagrams

Species	Chemical formula	ΔG_f^0 (kJ·mol^{-1})
1. Kaolinite	$Al_2Si_2O_5(OH)_4$	−3799.4
2. Pyrophyllite	$Al_2Si_4O_{10}(OH)_2$	−5265.9
3. Microcline	$KAlSi_3O_8$	−3742.3
4. Muscovite	$KAl_2(Si_3Al)O_{10}(OH)_2$	−5595.5
5. Water	H_2O	−237.1
6. Silicic acid	H_4SiO_4	−1309.2
7. Goethite	FeOOH	−488.7
8. Brucite	$Mg(OH)_2$	−833.5
9. Ferrous hydroxide	$Fe(OH)_2$	−492.0
10. Potassium ion	K^+	−282.7
11. Illite (Al)	$K_{0.75}Al_2(Si_{3.25}Al_{0.75})O_{10}(OH)_2$	−5508.9
12. Montmorillonite (Al)	$K_{0.3}Al_{1.9}Si_4O_{10}(OH)_2$	−5282.5
13. Illite (Mg)	$K_{0.75}Al_{1.75}Mg_{0.25}(Si_{3.50}Al_{0.50})O_{10}(OH)_2$	−5463.0
14. Montmorillonite (Mg)	$K_{0.30}Al_{1.70}Mg_{0.30}Si_4O_{10}(OH)_2$	−5308.3
15. Illite (Fe^{2+})	$K_{0.75}Al_{1.75}Fe_{0.25}(Si_{3.50}Al_{0.50})O_{10}(OH)_2$	−5376.7
16. Montmorillonite (Fe^{2+})	$K_{0.30}Al_{1.70}Fe_{0.30}Si_4O_{10}(OH)_2$	−5204.8
17. Illite (Fe^{3+})	$K_{0.75}Al_{1.6}Fe_{0.4}(Si_{3.25}Al_{0.75})O_{10}(OH)_2$	−5338.9
18. Montmorillonite (Fe^{3+})	$K_{0.30}Al_{1.5}Fe_{0.4}Si_4O_{10}(OH)_2$	−5112.4
19. Illite (Fe^{3+}, Mg)	$K_{0.75}Al_{1.35}Fe_{0.4}Mg_{0.25}(Si_{3.50}Al_{0.50})O_{10}(OH)_2$	−5293.0
20. Montmorillonite (Fe^{3+}, Mg)	$K_{0.30}Al_{1.3}Fe_{0.4}Mg_{0.30}Si_4O_{10}(OH)_2$	−5138.3
21. Erionite	$KAlSi_3O_8 \cdot 3H_2O$	−4458.7
22. Phillipsite	$K_3Al_3Si_5O_{16} \cdot 6H_2O$	−9240.6
23. Clinoptilolite	$KAlSi_5O_{12} \cdot 4H_2O$	−6406.5

Note: 1–3, 5, 7, 8, and 10—Robie et al. (1978). 4—Krupka et al. (1979). 6—Rimstidt (1984). 9—Nordstrom et al. (1984). 11–23—This model.

thermodynamic data are more accurate than these estimates and should be used in calculations when available. Furthermore, users should always consider whether the predictions of this approach make sense in terms of their geologic and/or geochemical experience.

The overall usefulness of this model is demonstrated by showing a few examples in the K_2O-Al_2O_3-SiO_2-H_2O system. These activity-activity diagrams show that the clay-mineral relations and the zeolite stability ranges determined using the estimated data agree well with experimental and geologic observations. Thus, the overall approach can be used to derive information on clay and zeolite mineral stabilities and then to develop a better understanding of chemical reactions that occur during diagenesis. The ΔG_r^0 values estimated from the model can be extrapolated to higher temperatures using estimated ΔH_r in the van't Hoff equation or by developing a similar model using higher-temperature experimental data. In addition, it is likely that this technique could successfully model the thermodynamic properties of other complex mineral families (e.g., sulfates, phosphates, arsenates, and vanadates). Finally, this research extends the use of the "polyhedral approach" (Hazen, 1988) in modeling the thermodynamic properties of silicate minerals from S^0 (Robinson and Haas, 1983; Holland, 1989) to include ΔG_f^0 and ΔH_f^0. The success of these "polyhedral models" strongly supports the concept that the properties of silicate minerals are mostly determined by nearest-neighbor interactions rather than by the longer-range ordering used to classify these minerals into structure types.

ACKNOWLEDGMENTS

Acknowledgment is made to the donors of The Petroleum Research Fund (PRF 18852-AC2), administered by the American Chemical Society, for partial support (95%), and to ARCO Oil and Gas Company. Critical reviews and comments by B. S. Hemingway, T.J.B. Holland, D. Langmuir, and Y. Tardy are gratefully acknowledged. R. J. Donahoe is thanked for the calorimetric data of merlionite.

REFERENCES CITED

Berman, R.G., Brown, T.H., and Greenwood, H.J. (1985) An internally consistent thermodynamic data base for the minerals in the system Na_2O-K_2O-CaO-MgO-FeO-Fe_2O_3-Al_2O_3-SiO_2-TiO_2-H_2O-CO_2. Atomic Energy of Canada Limited, Technical Report 377, 70 p.

Bloss, F.D., Gunter, M., Su, S.C., and Wolfe, H.E. (1983) Gladstone-Dale constants: A new approach. Canadian Mineralogist, 21, 93–99.

Carson, C.D., Kittrick, J.A., Dixon, J.B., and McKee, T.R. (1976) Stability of soil smectite from a Houston black clay. Clays and Clay Minerals, 24, 151–155.

Chaterjee, N. (1987) Evaluation of thermochemical data on Fe-Mg olivine, orthopyroxene, spinel, and Ca-Fe-Mg-Al garnet. Geochimica et Cosmochimica Acta, 51, 2515–2525.

Chen, C-H. (1975) A method of estimation of standard free energies of formation of silicate minerals at 298.15°K. American Journal of Science, 275, 801–817.

Clemens, J.D., Circone, S., Navrotsky, A., and McMillan, P.F. (1987) Phlogopite: High temperature solution calorimetry, thermodynamic properties, Al-Si and stacking disorder, and phase equilibria. Geochimica et Cosmochimica Acta, 51, 2569–2578.

Donahoe, R.J., Hemingway, B.S., and Liou, J.G. (1990a) Thermochemical data for merlinoite: I. Low-temperature heat capacities, entropies, and enthalpies of solution at 298.15 K of six synthetic samples having various Si/Al and Na/(Na + K) ratios. American Mineralogist, 75, in press.

Donahoe, R.J., Liou, J.G., and Hemingway, B.S. (1990b) Thermochemical data for merlinoite: II. Free energies of formation at 298.15 K of six synthetic samples having various Si/Al and Na/(Na + K) ratios. American Mineralogist, 75, in press.

Hay, R.L. (1986) Geologic occurrence of zeolites and some associated minerals. Pure and Applied Chemistry, 58, 1339–1342.

Hazen, R.M. (1985) Comparative crystal chemistry and the polyhedral approach. In S.W. Kieffer and A. Navrotsky, Eds., Microscopic to macroscopic: Atomic environments to mineral thermodynamics. Mineralogical Society of America Reviews in Mineralogy, 14, 317–345.

——— (1988) A useful fiction: Polyhedral modelling of mineral properties. American Journal of Science, 288-A, 242–269.

Hemingway, B.S. (1982) Thermodynamic properties of calcium aluminates. Journal of Physical Chemistry, 86, 2802–2803.

Hemingway, B.S., Haas, J.L., Jr., and Robinson, G.R., Jr. (1982) Thermodynamic properties of selected minerals in the system Al_2O_3-CaO-SiO_2-H_2O at 298.15 K and 1 bar pressure and at higher temperatures. U.S. Geological Survey Bulletin 1544.

Hemley, J.J., Montoya, J.W., Marinenko, J.W., and Luce, R.W. (1980) Equilibria in the system Al_2O_3-SiO_2-H_2O and some general implications for alteration/mineralization processes. Economic Geology, 75, 210–228.

Holland, T.J.B. (1989) Dependence of entropy on volume for silicate and oxide minerals: A review and a predictive model. American Mineralogist, 74, 5–13.

Huang, W.H., and Keller, W.D. (1973) Gibbs free energies of formation calculated from dissolution data using specific mineral analyses—III. Clay minerals. American Mineralogist, 58, 1023–1028.

Iijima, A. (1978) Geological occurrences of zeolite in marine environments. In L.B. Sand and F.A. Mumpton, Eds., Natural zeolites: Occurrence, properties and use, p. 175–198. Pergamon Press, New York.

Johnson, G.K., Flotow, H.E., and O'Hare, P.A.G. (1983) Thermodynamic studies of zeolites: Natrolite, mesolite and scolecite. American Mineralogist, 68, 1134–1145.

Johnson, G.K., Tasker, I.R., and Flotow, H.E. (1986) Thermodynamic studies of zeolites: Mordenite and dehydrated mordenite. Clay Mineral Society Abstracts, Jackson, Mississippi, p. 18.

Karpov, I.K., and Kashik, S.A. (1968) Computer calculation of standard isobaric-isothermal potentials of silicates by multiple regression from a crystallochemical classification. Geochemistry International, 5, 706–713.

Kittrick, J.A. (1971a) Stability of montmorillonites—I. Belle Fourche and clay spur montmorillonite. Soil Science Society of America Proceedings, 35, 140–145.

——— (1971b) Montmorillonite equilibria and the weathering environment. Soil Science Society of America Proceedings, 35, 815–820.

——— (1971c) Stability of montmorillonites—II. Aberdeen montmorillonite. Soil Science Society of America Proceedings, 35, 820–823.

——— (1982) Solubility of two high-Mg and two high-Fe chlorites using multiple equilibria. Clays and Clay Minerals, 30, 167–179.

——— (1984) Solubility measurements of phases in three illites. Clays and Clay Minerals, 32, 115–124.

Krupka, K.M., Robie, R.A., and Hemingway, B.S. (1979) High-temperature heat capacities of corundum, periclase, anorthite, $CaAl_2Si_2O_8$ glass, muscovite, pyrophyllite, $KAlSi_3O_8$ glass, grossular, and $NaAlSi_3O_8$ glass. American Mineralogist, 64, 86–101.

Kubaschewski, O., and Alcock, C.B. (1979) Metallurgical thermochemistry. Pergamon Press, Oxford.

La Iglesia, A., and Aznar, A.J. (1986) A method of estimating the Gibbs energies of formation of zeolites. Zeolites, 6, 26–29.

Makarov, T.I., Sidorov, Y.I., and Naumov, V.B. (1984) Formation conditions for iron minerals in ultrabasic-alkali metasomites. Geochemistry International, 21, 148–160.

Mattigod, S.V., and Sposito, G. (1978) Improved method for estimating the standard free energies of formation ($\Delta G_{f,298.15}$) of smectites. Geochimica et Cosmochimica Acta, 42, 1753–1762.

Misra, U.K., and Upchurch, W.J. (1976) Free energy of formation of beidellite from apparent solubility measurements. Clays and Clay Minerals, 24, 327–331.

Miyano, T., and Klein, C. (1983) Phase relations of orthopyroxene, olivine, and grunerite in high-grade metamorphic iron-formation. American Mineralogist, 68, 699–716.

Naumov, G.B., Ryzhenko, B.N., and Khodakovski, I.L. (1974) Handbook of thermodynamic data. National Technical Information Service, Report no. USGS-WRD-74-001, 328 p.

Nordstrom, D.K., Valentine, S.D., Ball, J.W., Plummer, L.N., and Jones, B.F. (1984) Partial compilation and revision of basic data in the WATEQ programs. U.S. Geological Survey Water-Resources Investigation Report 84-4186, 10–14.

Nriagu, J.O. (1975) Thermochemical approximations for clay minerals. American Mineralogist, 60, 834–839.

O'Hare, P.A.G., Johnson, G.K., Tasker, I.R., Howell, D.A., and Wise, W.S. (1986) Thermochemistry of geothermal materials. U.S. Department of Energy, Summaries of Physical Research in the Geosciences, 5–6.

Rimstidt, J.D. (1984) Quartz solubility at low temperatures. Geological Society of America Programs with Abstracts, 16, 635.

Robie, R.A., Hemingway, B.S., and Fischer, J.R. (1978) Thermodynamic properties of minerals and related substances at 298.15 K and 1 bar pressure and at higher temperatures. U.S. Geological Survey Bulletin 1452.

Robie, R.A., Bin, Z., Hemingway, B.S., and Barton, M.D. (1987) Heat capacity and thermodynamic properties of andradite garnet, $Ca_3Fe_2Si_3O_{12}$, between 10 and 1000 K and revised values for $\Delta_f G^0_m$ (298.15 K) of hedenbergite and wollastonite. Geochimica et Cosmochimica Acta, 51, 2219–2224.

Robinson, G.R., Jr., and Haas, J.L., Jr. (1983) Heat capacity, relative enthalpy, and calorimetric entropy of silicate minerals: An empirical method of prediction. American Mineralogist, 68, 541–553.

Sass, B.M., Rosenberg, P.E., and Kittrick, J.A. (1987) The stability of illite/smectite during diagenesis: An experimental study. Geochimica et Cosmochimica Acta, 51, 2103–2115.

Savin, S.M., and Lee, M. (1988) Isotopic studies of phyllosilicates. In S.W. Bailey, Ed., Hydrous phyllosilicates. Mineralogical Society of America, Reviews in Mineralogy, 19, 189–219.

Senkayi, A.L., Ming, D.W., Dixon, J.B., and Hossner, L.R. (1987) Kaolinite, opal CT, and clinoptilolite in altered tuffs interbedded with lignite in the Jackson Group, Texas. Clays and Clay Minerals, 35, 281–290.

Sheppard, R.A., and Gude, A.J., 3d. (1973) Zeolite and associated authigenic silicate minerals in tuffaceous of the Big Sandy Formation. U.S. Geological Survey Professional Paper 830.

Smyth, J.R., and Bish, D.L. (1988) Crystal structures and cation sites of the rock-forming minerals. Allen and Unwin, Boston.

Sposito, G. (1986) The polymer model of thermochemical clay mineral stability. Clays and Clay Minerals, 34, 198–203.

Stoessel, R.K. (1988) 25°C and 1 atm dissolution experiments of sepiolite and kerolite. Geochimica et Cosmochimica Acta, 52, 365–374.

Tardy, Y., and Garrels, R.M. (1974) A method of estimating the Gibbs energies of formation of layer silicates. Geochimica et Cosmochimica Acta, 38, 1101–1116.

——— (1976) Prediction of Gibbs energies of formation—I. Relationships among Gibbs energies of formation of hydroxides, oxides and aqueous ions. Geochimica et Cosmochimica Acta, 40, 1051–1056.

——— (1977) Prediction of Gibbs energies of formation—II. Monovalent and divalent metal silicates. Geochimica et Cosmochimica Acta, 41, 87–92.

Vieillard, Ph., and Tardy, Y. (1988) Estimation on enthalpies of formation of minerals based on their refined crystal structures. American Journal of Science, 288, 997–1040.

Wagman, D.D., Evans, W.H., Parker, V.B., Schumm, R.H., Halow, I., Bailey, S.M., Churney, K.L., and Nuttall, R.L. (1982) The NBS tables of chemical thermodynamic properties. Journal of Physical and Chemical Reference Data, 11.

Weaver, C.E., and Pollard, L.D. (1973) The chemistry of clay minerals. Elsevier, New York.

Zeng, Y., and Liou, J.G. (1982) Experimental investigation of yugawaralite-wairakite equilibrium. American Mineralogist, 67, 937–943.

Manuscript received November 14, 1988
Manuscript accepted May 17, 1989